MAUSAM, **54**, 1 (January 2003), 327-334

551.46 : 551.510.421

# Detection of marine aerosols using ocean colour sensors

INDRANI DAS and M. MOHAN

*Space Applications Centre, Ahmedabad - 380 015, India*

**e mail : mannilmohan@yahoo.com**

**सार** – महासागरीय रंगीन संवेदकों में स्पैकट्रस के अवरक्त क्षेत्र के निकट प्रचालित होने वाले वायुमंडलीय शोधन बैंड लगे हैं। इन तरंगदैर्ध्यों में, पानी के उच्च अवरक्त अवशोषण के कारण महासागरीय सतह एक गहरी पृष्ठभूमि के रूप में कार्य करती है और संवेदकों द्वारा पता लगाया गया विकिरण, वायुमंडलीय पवन अणु और एरोसोल्स, जिन्हें क्रमश : रेलै और एरोसोल मार्ग विकिरण कहा जाता है, द्वारा सौर विकिरण के पश्च प्रक्रीर्णन के कारण संभव हो पाता है। रेलै मार्ग विकिरण का हिसाब लगाने के उपरांत वायुमंडलीय शोधन बैंडों में विकिरणों से एरोसोल्स ऑप्टीकल डेप्थ (ए.ओ.डी.) और कण आकार वितरण सूची जैसे एरोसोल प्राचलों का पता लगाना संभव हुआ है।

ऑक्सीजन के विभेदक अवशोषण लक्षण का उपयोग करके लगभग 760 नॉटिकल मील $O_2$ A बैंड के चार संकीर्ण बैंड चैनलों में जहाँ आई.आर.एस. पी.3 एम.ओ.एस.–बी., आई.आर.एस. पी.4 ओ.सी.एम., एन.ओ.ए.ए.–ए.वी. एच.आर.आर. आदि जैसे संवेदक सकल वायुमंडलीय कॉलम में ए.ओ.डी. का पता लगाते हैं वहीं आई.आर.एस. पी.3 एम.ओ.एस–ए. सेंसर दो वायुमंडलीय स्तरों में ए.ओ.डी. का पता लगा सकते हैं। महासागरीय रंगीन संवेदकों से पता लगाने की पद्धति और आई.आर.एस. पी.3 एम.ओ.एस.–बी., आई. आर.एस. पी.4 – ओ.सी.एम. और आई आर. एस. पी. 3 एम.ओ.एस.–ए. विकिरण आँकड़ों से प्राप्त हुए परिणामों को इसमें प्रस्तुत किया गया और उस पर चर्चा की गई है।

**ABSTRACT.** Ocean colour sensors are equipped with atmospheric correction bands operating in the near infrared region of the spectrum. At these wavelengths, the ocean surface, because of high infrared absorption by water, acts as a dark background and the sensor detected radiance is due to solar radiation backscattered by the atmospheric air molecules and aerosols called Rayleigh and aerosol path radiances respectively. From the radiances in the atmospheric correction bands, after accounting for Rayleigh path radiance, it is possible to determine aerosol parameters like aerosol optical depth (AOD) and particle size distribution index.

While sensors like IRS P3 MOS-B, IRS P4 OCM, NOAA-AVHRR, etc detect AOD in the total atmospheric column, IRS P3 MOS-A sensor can detect AOD in two atmospheric layers by exploiting the differential absorption property of oxygen at four narrow band channels at the $O_2$ A band around 760nm. The method of determination from ocean colour sensors and the results from IRS P3 MOS-B, IRS P4-OCM and IRS P3 MOS-A radiance data are presented and discussed.

**Key words** – IRS P3 MOS-A & B, IRS P4 OCM, Atmospheric correction bands, Aerosol optical depth, Particle size distribution, Aerosol plumes, $O_2$ A absorption bands, Layer wise optical depth.

## 1. Introduction

Study of aerosols has gained greater importance in recent years with the increasing awareness of their radiative influence on the earth's atmosphere (Charlson *et al*., 1987). Aerosols are solid or liquid particles suspended in the air. Their sizes range from $\sim 10^{-2}$ to $10^{2}$ μm with the number density decreasing towards larger size. Large quantities of aerosols are continually being put into the atmosphere by natural and man made activities. Dust particles, soot particles, water-soluble particles, industrially produced sulphuric acid droplets, volcanic ash, etc. are some examples of aerosols (WCP, 1984). Aerosols have a wide range of chemical compositions resulting from the different mechanisms of their generation, *e.g.* wind blowing over deserts (silicate, mineral and clay particles), forest and man made fires (soot particles), volcanic eruptions (sulphate particles), vegetation (organic particles resulting from the photo chemical reaction of aromatic gases), industrial activities

(sulphates, nitrates, metallic particles), ocean waves (NaCl particles), oceanic phytoplankton (sulphate particles produced through the oxidation of dimethyl sulphide released during blooms, Kaufman *et al*., 1997), marine algae (photochemical reactions of iodine emissions from marine algae, Kolb, 2002) etc. Once released into the atmosphere, aerosols can remain in suspension for long periods of time: days to weeks in the case of tropospheric aerosols and months to years in the case of volcanic aerosols injected into the stratosphere by strong volcanic eruptions.

Aerosols are responsible for a variety of atmospheric effects: from causing reduced visibility, air pollution, acting as condensation nuclei in cloud formation, to modifying the weather and climate on a regional and global scales by affecting atmospheric radiation balance. Aerosols also interfere with the remote sensing activities requiring their effects to be eliminated from the radiance data of a sensor for the correct estimation of geophysical parameters. The most important among all the aerosol effects, however, is their role in the atmospheric radiation budget (Coakley *et al*., 1983) through scattering and absorption of the incident solar radiation. While they cool the earth's surface through scattering of solar radiation, the radiation absorbed by them warms the atmosphere.

In recent years, a number of attempts have been made to assess the impact of aerosols on the earth's weather and climate using numerical prediction models. Some studies have indicated on a global scale, their scattering effect can offset the greenhouse forcing by about 20-40% (WMO, 1996). Whereas on a regional scale, the numerical experiments show the aerosols to cause reduced vertical mixing in the tropics (through modification of the temperature profile), narrowing of the ITCZ (Inter Tropical Convergence Zone) and a slowing of the trade winds, cooling of the north Atlantic atmosphere and weakening the monsoon by reducing the land - sea temperature contrast. The results of such numerical experiments, though quantitatively uncertain, have provided important insights into aerosol effects in the atmospheric circulation dynamics. One major cause of the uncertainty is the lack of large scale information on aerosol parameters like their complex refractive indices, their seasonal variations, generation sources and sinks, vertical profile, residence time, etc. All the information currently available on aerosols are obtained mostly through land based observations (sun photometers, lidars, Anderson impactors, etc.) complemented by very rare observations on balloon borne, ship borne (Satheesh *et al*., 2001), aircraft borne and rocket borne platforms. These observations are of limited spatial and temporal extents highly inadequate for using as inputs into numerical prediction models.

Satellites, on the other hand, with their capability for large area coverage and short term repeativity, are the most ideal means for acquiring global information on aerosols. The satellite sensors SAM-I&II (Stratospheric Aerosol Measurement) and SAGE-I&II (Stratospheric Aerosol and Gas Experiment) have for several years (from late 70's to early 90's), monitored stratospheric aerosols through limb viewing sun occultation technique. However, these instruments did not have continuous spatial and temporal coverage and the measurements were confined to stratospheric altitudes.

The currently orbiting ocean colour sensors like IRS P3-MOS-B (Modular Optoelectronic Scanner), IRS P4-OCM (Ocean Colour Monitor) and SeaWiFS (Sea viewing Wide Field Sensor), though primarily meant for ocean colour sensing, can detect aerosols with large area coverage at frequent intervals. The prime mission of these sensors is to detect ocean water constituents (*e.g.* chlorophyll pigments, suspended particulate matter, yellow substance, etc.) from the solar radiation reflected by the upper layer of ocean in the spectral region ~ 400-700nm. But the radiation from seawater - called water leaving radiance - before reaching the space borne sensor, gets heavily contaminated by the solar backscatter from the atmospheric air molecules and aerosols. This atmospheric interference has to be removed from the sensor recorded radiances before they can be used for the estimation of ocean constituents. For this, every ocean colour sensor is additionally equipped with a few (a minimum of two) atmospheric correction channels or bands, which measure radiances in wavelengths greater than 700 nm. In these wavelengths, ocean surface acts as a dark background - because of high infrared absorption by water – and the detected radiances are just due to the solar backscatter produced in the atmosphere. Using the wave length dependence of this atmospheric radiance determined from the atmospheric correction bands, their values in the ocean colour wave lengths (below 700nm) are computed through an extrapolation and removed from the sensor measured radiances to obtain the water leaving radiances. The water leaving radiances are subsequently introduced into bio-geo-chemical algorithms for the estimation of ocean water constituents.

The atmospheric correction bands of the ocean colour sensors, while detecting atmospheric radiance, are also indirectly acquiring information on the atmospheric aerosols (Gordon, 1997) since part of the atmospheric radiance is produced by aerosol scattering. Therefore the radiances in the atmospheric correction channels become a means for detecting atmospheric aerosols over the oceans. The determination marine aerosol optical depth (AOD) and the index of their particle size distribution from the

**TABLE 1**

**Main specifications of some currently operational ocean colour sensors for aerosol detection**

| Sensor parameters | IRS P3-MOS-B | IRS P4-OCM | Sea WiFS | MODIS |
|---|---|---|---|---|
| Spatial resolution (km) | 0.52 | 0.360 | 1.1 | 1.0 |
| Swath (km) | 200 | 1420 | 2801 | 2330 |
| Repeativity (days) | 24 | 2 | 2 | 1 |
| Local time at equatorial crossing | 10:45 AM | 12 noon | 12 noon | 10:30 |
| Spectral bands (nm) | (1) 408±5 | (1) 412±10 | (1) 412±10 | (1) 412.5±7.5 |
| | (2) 443±5 | (2) 443±10 | (2) 443±10 | (2) 443±5 |
| | (3) 485±5 | (3) 490±10 | (3) 490±10 | (3) 488±5 |
| | (4) 520±5 | (4) 510±10 | (4) 520±10 | (4) 531±5 |
| | (5) 570±5 | (5) 555±10 | (5) 550±10 | (5) 551±5 |
| | (6) 615±5 | (6) 670±10 | (6) 670±10 | (6) 667±5 |
| | (7) 650±5 | (7) 765±20* | (7) 765±20* | (7) 678±5 |
| | (8) 685±5 | (8) 865±20* | (8) 865±20* | (8) 748±5* |
| | (9) 750±5* | | | (9) 869.5±7.5* |
| | (10) 815±5 | | | |
| | (11) 870±5* | | | |
| | (12) 945±5 | | | |
| | (13) 1010±5* | | | |
| Radiometric quantisation | 16 bits | 12 bits | 10 bits | 12 bits |
| Signal to Noise Ratio (SNR) | ~ 400 | ~ 350 | ~ 500 | ~1000 |

* indicates the bands used for aerosol detection

radiance data of atmospheric correction bands are described in section 2.

Based on the same principle, channels 1 and 2 of NOAA – AVHRR (550-680nm and 725-1100nm respectively) are currently being used for the detection and operational mapping of marine AOD. But unlike the bandwidths of ocean colour sensors (typically, 0-20nm), these channels are very broad and so, the aerosol information is likely to be contaminated by atmospheric water vapour absorption and scattering from suspended particulates in turbid coastal waters.

The MOS-A sensor on board the IRS P3 satellite has the capability to detect aerosols in two or three atmospheric layers through the differential absorption of solar radiation in four narrow band channels in the $O_2A$ (Oxygen) absorption band around 760 nm (Ding and Gordon, 1995). The basic technique of AOD detection by this sensor is described in section 3.

Results of AOD retrieval from IRS P4-OCM, IRS P3 MOS-A and B are presented in section 4 and the conclusions are discussed in section 5.

## 2. Aerosol parameters from ocean colour sensors

The main specifications of some of the currently operational ocean colour sensors MOS, OCM, SeaWiFS, MODIS (Moderate resolution Imaging Spectro radiometer) are given in Table 1

### 2.1. *Determination of aerosol optical depth (AOD)*

As stated section 1, water acts as a dark background for wavelengths λ >700nm because of high infrared absorption and so, the sensor detected radiance at the top of the atmosphere (TOA) will be just the sum of the radiances due to the scattering by air molecules (Rayleigh scattering) and aerosols (aerosols scattering) in the atmosphere. These radiances are also called the Rayleigh path radiance and the aerosol path radiance respectively. One can write,

$$L_t(\lambda) = L_r(\lambda) + L_a(\lambda) \quad (1)$$

where

$L_t$ = sensor detected TOA radiance in wave length λ

$L_{r,a} = F_0 w_{0r,a} \cdot \tau_{r,a} \cdot p_{r,a} / (4\pi\cos\theta_v)$
= Rayleigh/aerosol path radiance

$F_0$ = extra terrestrial solar flux

$\theta_v$ = satellite viewing zenith angle

$w_{0r}$ = Rayleigh single scattering albedo (~1.0)

$w_{0a}$ = aerosol single scattering albedo

$\tau_{r,a}$ = total column Rayleigh /aerosol optical depth

$p_{r,a}$ = *a* function related to the Rayleigh/aerosol scattering phase function

The function $p_{r,a}$ is related to the scattering phase function as

$$p_{a,r}(\gamma) = P_{a,r}(\gamma^-) + [R(\theta_v) + R(\theta_S)] P_{a,r}(\gamma^+) \quad (2)$$

where $R$ is the Fresnel reflectance of the water surface, $\theta_S$ is the solar zenith angle and $\gamma^{\pm}$is the forward/backward scattering angle defined by

$$\cos\gamma^{\pm} = \pm\cos\theta_V \cos\theta_S - \sin\theta_V \sin\theta_S \cos(\phi) \quad (3)$$

where $\theta_S$ is the sun zenith angle and $\phi$ is the azimuth difference between the sun illumination and satellite viewing directions. The Rayleigh optical depth at any wave length is determined by

$$\tau_r = 0.008735\ \lambda^{-4.08}\ (\sigma_a/1013.25) \quad (4)$$

where $\lambda$ is expressed in microns and $\sigma_a$ is the atmospheric pressure. The Rayleigh scattering phase function appearing in Eqn. (2) is given by

$$P_r(\gamma^{\pm}) = (3/4)[1 + \cos^2(\gamma^{\pm})] \quad (5)$$

The scattering phase function for aerosol $P_a(\gamma^{\pm})$ is approximated by a two term Heyney-Greenstein function (Das *et al*., 2002, Doerffer, 1992) defined by

$$P_a(\gamma^{\pm}) = Af(\gamma^{\pm}, g_1) + (1\text{-}A)\, f(\gamma^{\pm}, g_2) \quad (6)$$

where

$$f(\gamma^{\pm}, g) = (1 - g^2)/[(1 + g^2 - 2g\cos\gamma^{\pm})^{3/2}] \quad (7)$$

**TABLE 2**

**Main specifications of IRS P3 MOS-A**

| Sensor parameters | IRS P3-MOS-A |
|---|---|
| Spatial resolution (km) | 1.52 |
| Swath (km) | 200 |
| Repeativity (days) | 24 |
| Local time at equatorial crossing | 10:45 AM |
| Spectral bands (nm) | (1) 757.0±0.7 |
| | (2) 760.6±0.7 |
| | (3) 763.5±0.5 |
| | (4) 766.5±0.5 |
| Radiometric quantisation | 16 bits |
| Signal to Noise Ratio (SNR) | ~ 400 |

with $A$ = 0.985, $g_1$ = 0.8 and $g_2$ = 0.5 for marine aerosols (Sturm, 1980).

The relations (1) - (5) are used to determine the aerosol optical depth in an atmospheric correction band as

$$\tau_a = [(L_t - L_r)/F_0] \cdot 4\pi\cos\theta_v / p_a \quad (8)$$

in which $w_{0a}$ is assumed to be 1.0 for marine aerosols.

### 2.2. *Aerosol particle size distribution*

The aerosol optical depths derived using Eqn.(8) is related to the wavelengths of the atmospheric correction bands through the Angstrom's turbidity formula (Doerffer, 1992):

$$\tau_a = \text{const.}\ (\lambda)^{-\alpha} \quad (9)$$

where $\alpha$ is called the Angstrom exponent and can be determined as

$$\alpha = \frac{\log(\tau_{a1}) - \log(\tau_{a2})}{\log(\lambda_2) - \log(\lambda_1)} \quad (10)$$

The suffixes 1 and 2 correspond to the two atmospheric correction bands.

Based on large amount of observational data, Junge (1958) has proposed an aerosol particle size distribution in the form of a power law

$$dN/d(\log r) = C\, r^{-\nu} \quad (11)$$

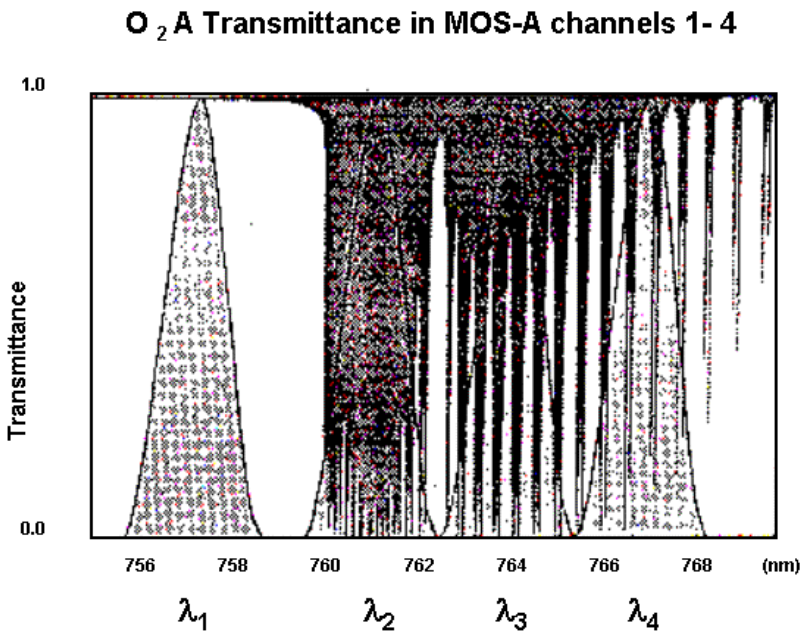


**Fig. 1.** Atmospheric transmittances in IRS P3 MOS-A channels 1-4

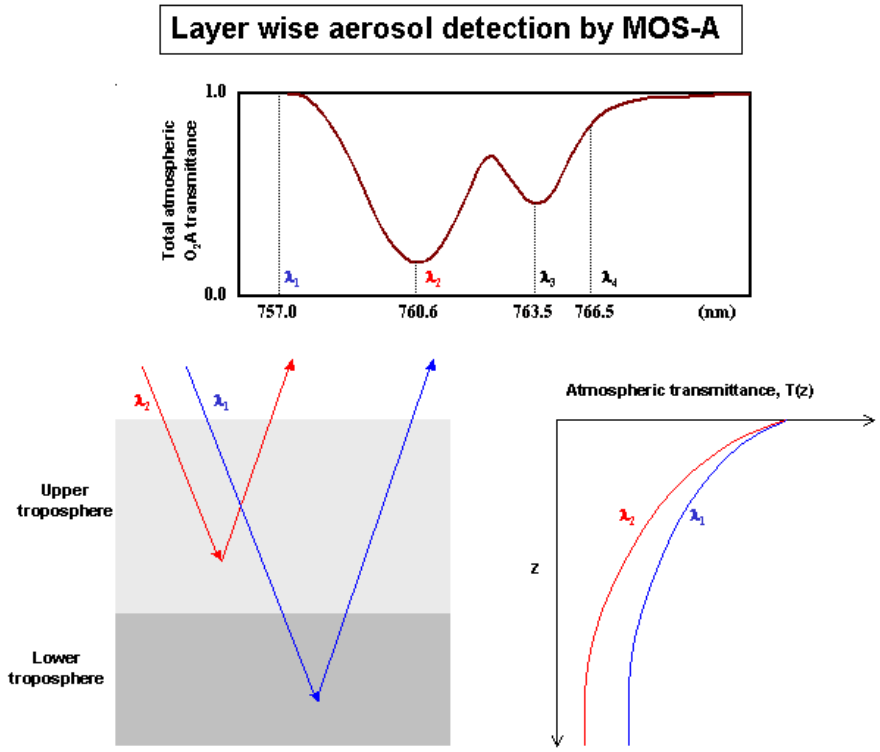


**Fig. 2.** The mechanism of layer wise detection of aerosols by MOS-A

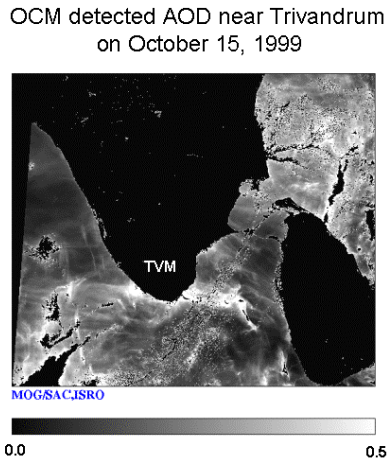


**Fig. 3.** Aerosol optical depth detected by IRS P4-OCM on 15 October, 1999, south of Trivandrum

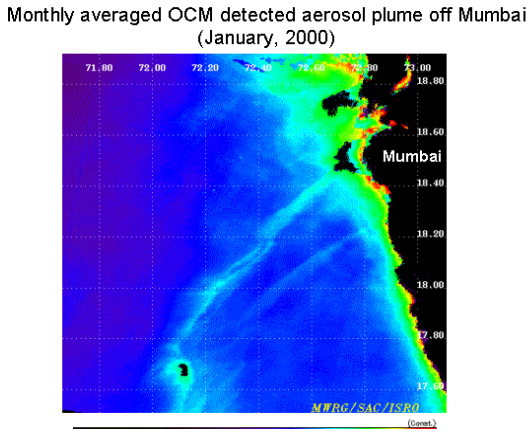


**Fig. 4.** Monthly averaged OCM detected AOD aerosol plume off Mumbai coast for January, 2000

where *dN* is the number of particles per unit volume with radii between *r* and *r* + d*r*, ν is the power law index and C is a constant. The index ν is related to the Angstrom exponent as,

$$\nu = \alpha + 2 \qquad (12)$$

One can see from relation (11) that as the value of ν (or α) increases, the particle size distribution becomes steeper and the number of smaller particles increases in comparison with larger particles making the average particle size smaller. Thus, larger values of Angstrom exponent can be taken to indicate a predominance of smaller particles and *vice versa*.

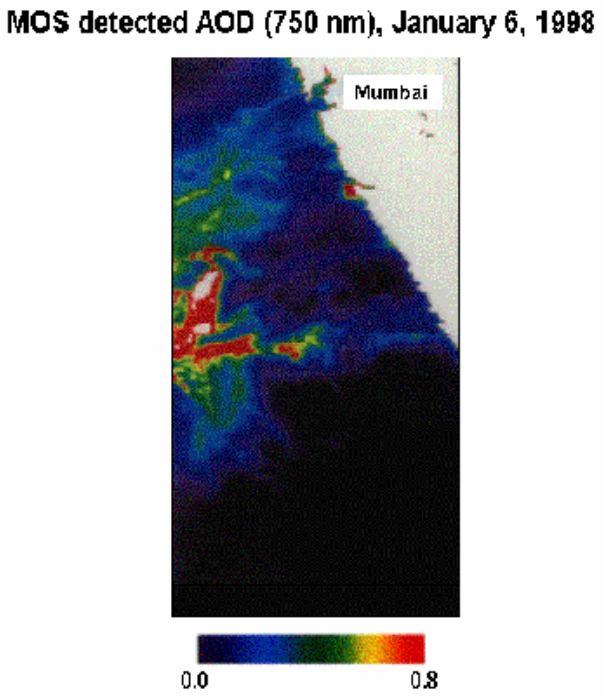


**Fig. 5.** Aerosols detected by IRS P3-MOS on 6 January 1998 seen giving rise to cloud formation acting as condensation nuclei

**TABLE 2**

**Main specifications of IRS P3 MOS-A**

| Sensor parameters | IRS P3-MOS-A |
|---|---|
| Spatial resolution (km) | 1.52 |
| Swath (km) | 200 |
| Repeativity (days) | 24 |
| Local time at equatorial crossing | 10:45 AM |
| Spectral bands (nm) | (1) 757.0±0.7<br>(2) 760.6±0.7<br>(3) 763.5±0.5<br>(4) 766.5±0.5 |
| Radiometric quantisation | 16 bits |
| Signal to Noise Ratio (SNR) | ~ 400 |

## 3. Detection of AOD in two atmospheric layers by MOS-A

The main specifications of the MOS-A sensor on board IRS P3 are given in Table 2. It has the capability for layer wise detection of aerosols by utilising the differential nature of the $O_2$A absorption of atmospheric oxygen in four narrow band channels (Fig. 1).

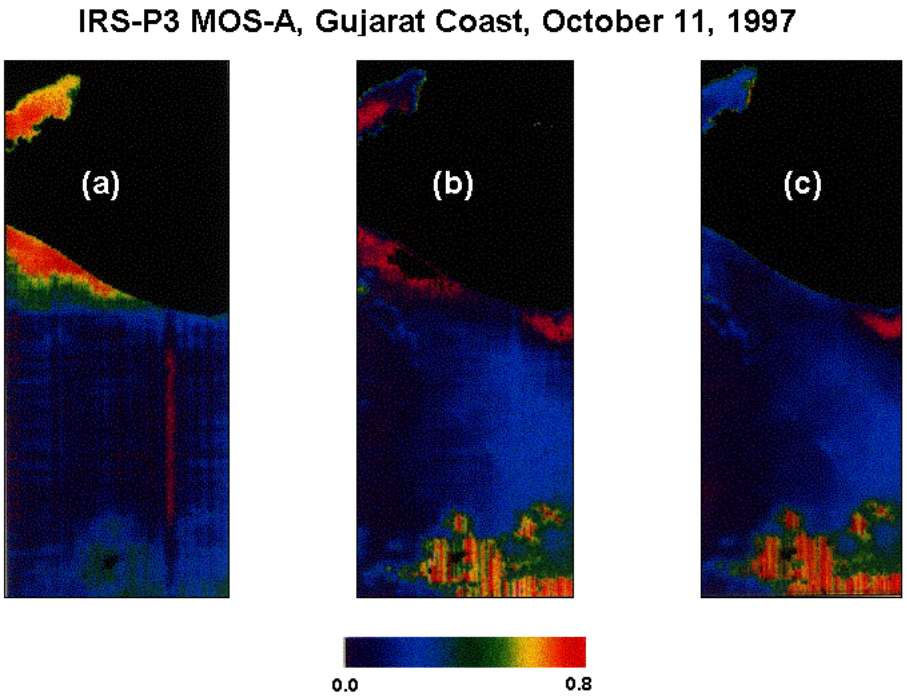


**Figs. 6 (a-c).** Aerosol distribution in two layers detected by IRS P3-MOS. (a) Aerosol optical depth in the top (3-9 km) layer (enhanced by a factor of 10) (b) Aerosol optical depth in the boundary layer (0-3 km) and (c) Total columnar aerosol optical depth

The basic idea involved here, as depicted in Fig. 2, is that the light backscattered by aerosols in the upper and the lower layers travel different distances in the atmosphere decided by the strength of absorption in the different MOS-A channels. Consequently, the channel with maximum absorption will contain radiation scattered by aerosols predominantly in the upper layer while the channels with weak absorption will contain radiation scattered by aerosols in the upper as well as lower layers. Therefore, from the radiances measured in a few channels (say, three or four) with varying degrees of absorption, it is possible to separate out aerosols in two or three layers through an inversion procedure after accounting for the reflectance from the ocean surface.

### 3.1. *Formulation of the inversion problem*

The radiance detected in the $i^{th}$ MOS-A channel is given by the following integral:

$$L_{ti} = [F_{0i}/(4\pi\cos\theta_v)] \int_0^\infty K^0{}_2(\lambda_i,z).x_i(z)\, dz + \delta L_i \qquad (13)$$

where

$K^0{}_2$ $(\lambda_i,z)$ = kernel representing the $O_2$A transmittance

$$x_i = \{[d\tau_{ri}(z)/dz]w_{0ri}p_{ri}+[d\tau_{ai}(z)/dz]w_{0ai}p_{ai}\}.$$
$$\exp\ \{-s[\tau_{ri}(z)+\tau_{ai}(z)]\} \qquad \text{for } z > 0$$

$$= 4\pi\, R(\theta_s, \theta_v)\cos\theta_s.\exp\{-s[\tau_{ri}(0)+\tau_{ai}(0)]\}$$
$$\text{for } z = 0$$

$R(\theta_s, \theta_v)$= ocean surface reflectance

$s = 1/\cos\theta_v + 1/\cos\theta_s$

$\delta L_i$ = noise in the $i^{th}$ channel

Taking a simple, two layer model for the atmosphere with one layer between 0 and 3 km (boundary layer) and a second layer between 3 and 9 km (upper tropospheric layer) with aerosol optical depths $\tau_{a1}$ and $\tau_{a2}$ for the upper and the lower layers respectively, one can use Eqn.(13) to write the aerosol path radiance as,

$$L_{ai} = A_i\tau_{a1}T_i(1) + B_i\tau_{a2}T_i(1,2) + R\,T_{si}(1,2) + L_{ri} \qquad (14)$$

where $i$=1,2 correspond to the least and the maximum absorption channels, $A_i$ and $B_i$ are functions of the extra terrestrial flux, viewing angle, aerosol scattering phase functions and the aerosol single scattering albedo, $T_i(1)$ is

a function of $\tau_{a1}$, $T_i(1,2)$ and $T_{si}(1,2)$ are functions of $\tau_{a1}$ and $\tau_{a2}$ and $L_{ri}$ is the Rayleigh path radiance.

## 4. Results

Fig. 3 is an IRS P4-OCM image showing the total column AOD distribution near Trivandrum in the month on 15 October, 1999. One can notice in this image streaks of aerosols caused by the extending from the land to the oceans in various directions caused by the prevailing winds at the time of satellite pass. The dark patches are areas the masked for highly reflecting land and cloud surfaces. While land surface has sharp edges, the clouds have optically thin parts near the edges which are not masked.

The monthly averaged AOD derived from OCM for January 2000 is shown in Fig. 4. A intense plume of aerosols from Mumbai coast, probably generated by the industrial activities, is found to extend deep into the ocean under the influence of the northwesterly winds of the season.

Fig. 5 is MOS-B AOD image of aerosol plume from Mumbai coast on 6 January, 1998 seen connected to a large patch of cloud. This is a typical example of aerosols acting as condensation nuclei giving rise to cloud formation.

Figs. 6 (a-c) show the layer wise distribution of aerosols detected by IRS P3 MOS-A sensor off the Gujarat coast on 11 October, 1997. Fig. 5(a) shows the AOD (scaled up by a factor 10) in the top (or 3-9km) layer, (b) represents the boundary (0-3km) layer and (c) is the total columnar aerosol optical depth.

## 5. Summary and conclusions

Satellites are one of the most effective means for global monitoring of aerosols at frequent intervals. The atmospheric correction bands of space borne ocean colour sensors can provide quantitative information aerosol parameters such as aerosol optical depth and size distribution index. Results from the ocean colour sensors IRS P3 MOS-B and IRS P4-OCM are presented. It was seen that these sensors can detect the aerosol origins near the coast and the extent of their dispersal into the oceanic atmosphere.

The differential absorption property of IRS P3 MOS-A channels near the $O_2$A band was used to estimate AOD in two atmospheric layers. This can be an effective tool in studying the transport of aerosols governed by the winds in the upper and lower tropospheric altitudes.

### References


Charlson, R., Lovelock, J., Andreae, M. and Warren, S., 1987, "Oceanic phytoplankton, atmospheric sulpher, cloud albedo and climate", *Nature*, **326**, 655-661.

Coakley, J. A., Cess, R. D. and Yurevich, 1983, "The effect of tropospheric aerosols on the earth's radiation budget: A parameterisation for climate models", *J. Atmos. Sci*., **40**, 116-138.

Das, Indrani, Mohan, M. and Krishnamoorthy, K., 2002, "Detection of marine aerosols with IRS P4-Ocean Colour Monitor", Proceedings, *Indian Aca. of Sciences* (in press).

Ding, K. and Gordon, H. R., 1995, "Analysis of the influence of $O_2$A band absorption on atmospheric correction of ocean colour imagery", *Appl. Opt*., **34**, 2068-2080.

Doerffer, R., 1992, "Imaging spectroscopy for detection of chlorophyll and suspended matter", GKSS 92/E/54, GKSS-FORSCHUNGSZENTRUM GEESTHACHT GMBH.

Gordon, H. R., 1997, "Atmospheric correction of ocean colour imagery in the Earth Observing System era", *J. Geophys. Res*., **102**, 17081-17106.

Junge, C. E., 1958, "Atmospheric Chemistry", *Adv. Geophys*., **4**, 1-108.

Kaufman, Y. J., Tanre, D., Gordon, H. R., Nakajima, T., Lenoble, J., Frouin, R., Grassl, H., Herman, B. M., King, M. D. and Teillet, P. M., 1997, "Passive remote sensing of tropospheric aerosol and atmospheric correction for the aerosol effect", *J. Geophys. Res*. **102**, D14, 16815-16830.

Kolb, C. E., 2002, "Iodine's air of importance", *Nature*, **417**, 597-598.

Satheesh, S. K., Krishnamoorthy, K. and Indrani Das, 2001, "Aerosol spectral optical depths over Bay of Bengal, Arabian Sea and Indian Ocean", *Current Science*, **81**, 12, 1617-1627.

Sturm, B., 1980, "The Atmospheric Corrections of Remotely Sensed Data and the Qualitative determination of Suspended Matter In Marine Water Surface layers", A. P. Cracknell (ed.), Remote sensing in Meteorology, Oceanography and Hydrology, Ellis Horwood Ltd., Chichester, 163-197.

WCP (World Climate Programme), 1984, "A preliminary cloudless standard atmosphere for radiation computation", Radiation Commission, Boulder, USA.

WMO (World Meteorological Organisation), 1996, "WMO & Climate change", WMO Rep. No. 848.